ELSEVIER

Polymer 43 (2002) 4063–4071

polymer

www.elsevier.com/locate/polymer

Molecular orientation and stress in biaxially deformed polymers. II. Steady potential flow

Leszek Jarecki*, Andrzej Ziabicki

Institute of Fundamental Technological Research, Polish Academy of Sciences, Swietokrzyska 21, 00-049 Warsaw, Poland

Received 8 January 2002; received in revised form 6 March 2002; accepted 6 March 2002

Abstract

The development of biaxial segmental orientation and stress in a flexible-chain polymer fluid subjected to steady biaxial extensional flow is analyzed. Closed-formula model based on the Padè approximation of the inverse Langevin function in the non-Gaussian distribution of the chain end-to-end vectors is considered. The approach is free from the limitations related to finite chain extensibility and slow convergence of the series expansion formulations at higher chain deformations.

Segmental orientation is characterized by the average orientation tensor, related axial orientation factors and global orientation anisotropy. Orientational behavior and corresponding stresses in the biaxial elongational potential flow are discussed in a wide range of elongation rates. Orientation characteristics calculated for the biaxial flow deformation are much higher than those predicted for the affine biaxial stretch deformation in polymer solids.

Keywords: Biaxial molecular orientation; Axial orientation factor; Orientation anisotropy

1. Introduction

An increasing interest in the formation of high-performance films from flexible-chain polymers led several authors to experimental [1–8] and theoretical [1,6,9–11] investigations on the characterization and development of biaxial orientation. In theoretical modeling of formation of high molecular orientation, applicability of Gaussian chain statistics is limited by finite extensibility of the polymer chains, in particular at higher molecular deformations. On the other hand, series expansion theories involving non-Gaussian chain statistics lead at higher molecular deformations to weekly converging formulations [10,11].

In a recent paper [11] we have applied a Padè approximation of the inverse Langevin function in so-called inverse Langevin distribution of chain conformations. This led us to a closed-formula theory for the entire range of chain extensions. In Ref. [11], we discuss molecular orientation and stresses in systems subjected to affine biaxial deformation in solid polymers. Affine deformation of polymer chains is introduced by a macroscopic deformation of polymer network or by a plastic deformation of uncrosslinked solids.

An alternative way of introducing molecular deformation and orientation is an orienting potential flow applied to systems with high molecular mobility, like polymer melts or concentrated solutions. Unlike in solid-state, molecular deformation and orientation in a viscous fluid are controlled by deformation rate (or stress) implied by the flow, rather than by deformation. This picture seems to be confirmed by the orientation behavior in Nylon 6 fibers, either cold-drawn in a plastic state where the orientation is controlled by the draw ratio, or melt-spun where the orientation is controlled by the spinning speed (or spinning stress) [12,13].

In more complex, viscoelastic materials, effects of deformation and deformation rate are superimposed one on another. Melt spinning of highly viscoelastic polyethylene shows both, deformation (spin–draw ratio) as well as deformation rate (spinning speed) effects.

In this paper, we analyze the development of molecular orientation and stress in a viscous fluid subjected to steady, biaxial extensional flow. We use the Padè approximation of the inverse Langevin function [14] in the non-Gaussian distribution of the chain end-to-end vectors. The results should be relevant to such fluid state industrial processes as melt spinning of fibers, melt blowing or solution casting of films, etc. Transient viscoelastic effects will be discussed in separate papers.

* Corresponding author. Tel.: +48-22-827-8182; fax: +48-22-826-9815.
E-mail address: ljarecki@ippt.gov.pl (L. Jarecki).

0032-3861/02/$ - see front matter
PII: S0032-3861(02)00231-8

2. Molecular orientation and stress in systems of flexible polymer chains

Like in the previous paper, we consider a non-Gaussian, freely jointed polymer chains, whose unperturbed end-to-end vectors' distribution is described by the inverse Langevin statistics [15]

$$W_0(\mathbf{h}) = \text{const.}\exp\left[-N\int_0^{h/Na}\mathscr{L}^*(x)\mathrm{d}x\right] \tag{1}$$

where a is a fixed-length statistical Kuhn segment, N, the number of such segments in a chain.

Series expansion of the inverse Langevin function assumes the form

$$\mathscr{L}^*(x) = 3x + \frac{9}{5}x^3 + \frac{297}{175}x^5 + \frac{1539}{875}x^7 + \frac{126117}{67375}x^9 + \cdots \tag{2}$$

Function $\mathscr{L}^*(x)$ can be effectively described by its Padè approximation in the following form [14]

$$\mathscr{L}^*(x) = x\frac{3-x^2}{1-x^2} \tag{3}$$

applicable in the entire range of variable x.

The expanded form of the unperturbed distribution of the end-to-end vector $\mathbf{h}$ reads

$$W_0(\mathbf{h}) = \text{const.}\exp\left\{-\frac{3h^2}{2Na^2}\left[1+\frac{3}{10}\left(\frac{h}{Na}\right)^2 + \frac{33}{175}\left(\frac{h}{Na}\right)^4 + \frac{513}{3500}\left(\frac{h}{Na}\right)^6 + \frac{42039}{336875}\left(\frac{h}{Na}\right)^8 + \cdots\right]\right\} \tag{4}$$

and with the Padè approximation

$$W_0(\mathbf{h}) \cong \text{const.}\left[1-\left(\frac{h}{Na}\right)^2\right]^N \exp\left(-\frac{h^2}{2Na^2}\right) \tag{5}$$

The distributions (4) and (5) are functions of the chain extension h/Na and N.

Equilibrium orientation distribution of the chain segments around the end-to-end vector $\mathbf{h}$ is cylindrically symmetric, and is characterized by the normalized distribution of the cosine of angle α between a segment and the vector $\mathbf{h}$ [16]

$$w_{s0}(\cos\alpha) = \frac{\mathscr{L}^*(h/Na)}{4\pi\ \mathrm{sh}[\mathscr{L}^*(h/Na)]}\exp\left[\mathscr{L}^*\left(\frac{h}{Na}\right)\cos\alpha\right] \tag{6}$$

The distribution w_{s0} can be considered as a conditional probability of finding statistical segment oriented at the angle α (with respect to vector $\mathbf{h}$) at fixed chain extension h/Na.

Orientation of segments in a single polymer chain with end-to-end vector $\mathbf{h}$ is represented by the following orientation tensor [16], controlled only by the chain extension h/Na

$$\mathbf{A}(\mathbf{h}) = \left[1-\frac{3\frac{h}{Na}}{\mathscr{L}^*\left(\frac{h}{Na}\right)}\right]\frac{\mathbf{h}\otimes\mathbf{h}}{h^2} = \left[\frac{3}{5}\left(\frac{h}{Na}\right)^2 + \frac{36}{175}\left(\frac{h}{Na}\right)^4 + \frac{108}{875}\left(\frac{h}{Na}\right)^6 + \frac{5508}{67375}\left(\frac{h}{Na}\right)^8 + \cdots\right]\frac{\mathbf{h}\otimes\mathbf{h}}{h^2} \tag{7}$$

With the Padè approximation the orientation tensor reduces to

$$\mathbf{A}(\mathbf{h}) \cong \frac{2}{3(Na/h)^2-1}\frac{\mathbf{h}\otimes\mathbf{h}}{h^2} \tag{8}$$

The number of chain configurations available at fixed vector $\mathbf{h}$ is proportional to the unperturbed, equilibrium distribution function $W_0(\mathbf{h})$. The entropy of the chain composed of N statistical segments is given by

$$S(\mathbf{h}) = k\ln W_0(\mathbf{h}) = \text{const.} - Nk\int_0^{h/Na}\mathscr{L}^*(x)\mathrm{d}x \tag{9}$$

With the series expansion (2), the chain entropy reads

$$S(\mathbf{h}) = \text{const.} - \frac{3Nk}{2}\left[1+\frac{3}{10}\left(\frac{h}{Na}\right)^2 + \frac{33}{175}\left(\frac{h}{Na}\right)^4 + \frac{513}{3500}\left(\frac{h}{Na}\right)^6 + \frac{42039}{336875}\left(\frac{h}{Na}\right)^8 + \cdots\right]\left(\frac{h}{Na}\right)^2 \tag{10}$$

and with the Padè formula

$$S(\mathbf{h}) \cong \text{const.} - Nk\left[\frac{1}{2}\left(\frac{h}{Na}\right)^2 - \ln\left(1-\left(\frac{h}{Na}\right)^2\right)\right] \tag{11}$$

The 'local' molecular stress tensor corresponding to the elastic force between the chain ends reads [17,18]

$$\mathbf{p} = \frac{1}{Nv_0}\mathbf{f}\otimes\mathbf{h} = \frac{kT}{v_0}\left(\frac{h}{Na}\right)\mathscr{L}^*\left(\frac{h}{Na}\right)\frac{\mathbf{h}\otimes\mathbf{h}}{h^2} \tag{12}$$

where v_0 denotes volume per single segment.

Using the expansion formula (2) one obtains

$$\mathbf{p}(\mathbf{h}) = \frac{3kT}{v_0}\left[1+\frac{3}{5}\left(\frac{h}{Na}\right)^2 + \frac{99}{175}\left(\frac{h}{Na}\right)^4 + \frac{513}{875}\left(\frac{h}{Na}\right)^6 + \frac{42039}{67375}\left(\frac{h}{Na}\right)^8 + \cdots\right]\frac{\mathbf{h}\otimes\mathbf{h}}{N^2a^2} \tag{13}$$

and with the Padè approximation we have

$$\mathbf{p} \cong \frac{kT}{v_0}\left(\frac{h}{Na}\right)^2\left[\frac{3-\left(\frac{h}{Na}\right)^2}{1-\left(\frac{h}{Na}\right)^2}\right]\frac{\mathbf{h}\otimes\mathbf{h}}{h^2} \tag{14}$$

In both expressions, the molecular stress tensor **p** depends, except for temperature, only on the chain extension h/Na.

Global orientation distribution of the segments in the system of chains, $w_s(\theta,\varphi)$, is obtained from the integral

$$w_s(\theta,\varphi) = \int w_{s0}\left(\frac{\mathbf{a}\cdot\mathbf{h}}{ah}\right)W(\mathbf{h})d^3\mathbf{h} \tag{15}$$

where $\mathbf{a}\cdot\mathbf{h}/(ah) = \cos\alpha$. θ, φ denote polar angles of the segment vector **a** in an external coordinate system. $W(\mathbf{h})$ is the actual distribution of end-to-end vectors in the deformed system.

Time-dependent distribution function of end-to-end vectors, $W(\mathbf{h},t)$, in the system subjected to the flow deformation can be found from the following continuity equation [11,18]

$$\frac{\partial W}{\partial t} + \mathrm{div}\left[W\dot{\mathbf{h}}_0 - D\left(\nabla W + W\nabla\frac{F_{el}}{kT}\right)\right] = 0 \tag{16}$$

where F_{el} is entropy-controlled elastic free energy between the chain ends, D the diffusion coefficient of the chain end point. The chain can be represented here by a Brownian dumbbell with a non-Hookean elastic potential, subjected to the flow.

The convective deformation rate of a chain end-to-end vector in the flow, $\dot{\mathbf{h}}_0$, is characterized by the macroscopic velocity gradient tensor $\nabla\mathbf{V}$, equal in the case of extensional flow to the deformation rate tensor **Q**

$$\dot{\mathbf{h}}_0 = \nabla\mathbf{V}\cdot\mathbf{h} \tag{17}$$

$$\nabla\mathbf{V} = \mathbf{Q} = \frac{1}{2}(\nabla\mathbf{V} + \nabla\mathbf{V}^{\mathrm{T}}) \tag{18}$$

We consider diagonal velocity gradient tensor, constant in time

$$\nabla\mathbf{V} = \mathbf{Q} = \begin{bmatrix} q_1 & 0 & 0 \\ 0 & q_2 & 0 \\ 0 & 0 & q_3 \end{bmatrix} \tag{19}$$

In the previous paper [11], we have analyzed an asymptotic solution of Eq. (16) in the limit of infinitely small molecular mobility, D. The limit corresponds to the solid-state behavior, and molecular orientation and stress are controlled by global, macroscopic deformation of the system. In this paper, we consider another special solution, corresponding to a viscous fluid.

3. Equilibrium distribution in steady potential flow

Another asymptotic case is obtained as an 'equilibrium' orientation distribution in the potential flow. Using the idea of Kramers [19,20] applied in our earlier papers [18,21] we consider the effect of steady potential flow as an additional scalar thermodynamic potential. The flow potential $H(\mathbf{h})$ satisfies the following equations

$$H(\mathbf{h}) = \frac{1}{2}\mathbf{h}\cdot\dot{\mathbf{h}}_0 = \frac{1}{2}\mathbf{h}\cdot\mathbf{Q}\mathbf{h} \tag{20}$$

$$\nabla H(\mathbf{h}) = \dot{\mathbf{h}}_0 = \mathbf{Q}\mathbf{h} \tag{21}$$

$$\nabla\nabla^{\mathrm{T}}H(\mathbf{h}) = \mathbf{Q} = \text{const.} \tag{22}$$

and can be combined with the elastic free energy of the chain, $F_{el}(\mathbf{h})$. For a steady-state potential flow Eq. (16) reduces to a simple first-order differential equation

$$\nabla W + W\nabla\left[\frac{F_{el}(\mathbf{h})}{kT} - \frac{H(\mathbf{h})}{D}\right] = 0 \tag{23}$$

yielding equilibrium distribution in the Boltzmann form

$$W(\mathbf{h}) = \text{const.}\exp\left[-\frac{F_{el}(\mathbf{h})}{kT} + \frac{H(\mathbf{h})}{D}\right] \tag{24}$$

Introducing the molecular friction coefficient ζ and the relaxation time τ, inversely proportional to the diffusion coefficient D

$$\zeta = \frac{6kT\tau}{Na^2} = \frac{kT}{D} \tag{25}$$

and the elastic free energy

$$F_{el}(\mathbf{h}) = -kT\ln W_0(\mathbf{h}) = NkT\int_0^{h/Na}\mathscr{L}^*(x)\mathrm{d}x \tag{26}$$

we obtain the following equilibrium orientation distribution of the end-to-end vectors

$$W(\mathbf{h},\mathbf{Q}) = \text{const.}\exp\left[-N\int_0^{h/Na}\mathscr{L}^*(x)\mathrm{d}x + 3\tau\frac{\mathbf{h}\cdot\mathbf{Q}\mathbf{h}}{Na^2}\right] \tag{27}$$

In the Gaussian approximation, the normalized distribution of vector **h** in the flow reduces to the form

$$\begin{aligned} W(\mathbf{h},\mathbf{Q}) &= \left(\frac{3}{2\pi Na^2}\right)^{3/2}[(1-2\tau q_1)(1-2\tau q_2) \\ &\times(1-2\tau q_3)]^{1/2}\exp\left\{-\frac{3}{2Na^2}\left[(1-2\tau q_1)h_1^2\right.\right. \\ &\left.\left.+(1-2\tau q_2)h_2^2+(1-2\tau q_3)h_3^2\right]\right\} \\ &= \left(\frac{3}{2\pi Na^2}\right)^{3/2}(\det\Gamma_{\mathrm{H}})^{-3/2}\exp\left(-\frac{3}{2Na^2}\mathbf{h}\cdot\Gamma_{\mathrm{H}}^{-1}\mathbf{h}\right) \end{aligned} \tag{28}$$

where the tensor Γ_H describes an equilibrium molecular deformation of the end-to-end vectors of Gaussian chains in the flow

$$\Gamma_H = \begin{bmatrix} \frac{1}{1-2\tau q_1} & 0 & 0 \\ 0 & \frac{1}{1-2\tau q_2} & 0 \\ 0 & 0 & \frac{1}{1-2\tau q_3} \end{bmatrix} \tag{29}$$

The molecular deformation tensor Γ_H substantially differs from the macroscopic flow deformation tensor $\exp(\mathrm{tr}\,\mathbf{Q}t)$. Distribution function (28) becomes undefined at the extension rates $\tau q_i \geq 1/2$ ($i = 1$, 2, or 3) and principal components of Γ_H also reflect the indeterminacy of chain deformation under such flow.

In the case of Gaussian chains, the equilibrium distribution of **h** vectors in the flow corresponds to an affine distribution controlled by the deformation tensor Γ_H. Such a behavior is a direct consequence of linearity of the flow and Gaussian elastic potentials. Non-linear elasticity of non-Gaussian chain deviates the distribution from an affine-type, and tensor Γ_H does no longer characterize chain deformation, in particular at higher values of τq_i.

With the Padè approximation, we receive the distribution function of chain end-to-end vectors in the following closed form

$$W(\mathbf{h},\mathbf{Q}) \cong \text{const.}\left[1-\left(\frac{h}{Na}\right)^2\right]^N \exp\left\{-\frac{1}{2Na^2} \times\left[(1-6\tau q_1)h_1^2+(1-6\tau q_2)h_2^2+(1-6\tau q_3)h_3^2\right]\right\} \tag{30}$$

without any indeterminacy in the entire range of the reduced extension rates τq_i, and no affine-type distribution of the chain end-to-end vectors can be introduced.

Integration of the intra-chain orientation distribution of the statistical Kuhn segments $w_{s0}(\alpha)$ with the distribution (27) yields global orientation distribution of the chain segments. The approximate Gaussian form, controlled by tensor Γ_H and obtained from the combination of the linearized form of Eq. (6) with Eq. (28), reads

$$w_s(\theta,\varphi) \cong \frac{1}{4\pi}\left\{1-\frac{1}{2}\mathrm{tr}\left(\frac{\Gamma_H}{N}\right)\right\}\exp\left(\frac{3}{2}\frac{\mathbf{a}\cdot\Gamma_H\mathbf{a}}{Na^2}\right) \tag{31}$$

where the Gaussian angular distribution of Kuhn segments is controlled by

$$\frac{\mathbf{a}\cdot\Gamma_H\mathbf{a}}{Na^2} = \frac{1}{N}\left[\left(\frac{1}{1-2\tau q_1}\cos^2\varphi+\frac{1}{1-2\tau q_2}\sin^2\varphi\right)\sin^2\theta + \frac{1}{1-2\tau q_3}\cos^2\theta\right] \tag{32}$$

and scaled by the inverse number of the segments in a chain, N^{-1}. The approximation can be used for small values of the reduced flow rates τq_i. In the absence of flow ($H = q_1 = q_2 = q_3 = 0$), the orientation distribution reduces to uniform.

4. Average behavior in flowing systems

Average values of the entropy, orientation and molecular stress tensors in the system subjected to the flow are obtained by integration of the functions with actual distribution of the end-to-end vectors, $W(\mathbf{h})$

$$\langle S\rangle = \int S(\mathbf{h})W(\mathbf{h})d^3\mathbf{h} \tag{33}$$

$$\langle \mathbf{A}\rangle = \int \mathbf{A}(\mathbf{h})W(\mathbf{h})d^3\mathbf{h} \tag{34}$$

$$\langle \mathbf{p}\rangle = \int \mathbf{p}(\mathbf{h})W(\mathbf{h})d^3\mathbf{h} \tag{35}$$

For the equilibrium Gaussian distribution of the chains, applicable to relatively small molecular deformations ($\tau q_i \ll 1/2$), one obtains

$$\frac{\langle S\rangle}{kN} = \text{const.} - \frac{1}{2N}\left[\frac{1}{1-2q_1\tau}+\frac{1}{1-2q_2\tau}+\frac{1}{1-2q_3\tau}\right] = \text{const.} - \frac{1}{2}\mathrm{tr}\frac{\Gamma_H}{N} \tag{36}$$

$$\langle \mathbf{A}\rangle = \frac{1}{5}\frac{\Gamma_H}{N} \tag{37}$$

$$\frac{\langle \mathbf{p}\rangle v_0}{kT} = \frac{\Gamma_H}{N} \tag{38}$$

The effects of flow deformation on the average entropy per single segment, average molecular orientation and stress tensors scale with the inverse number of segments in a chain, N^{-1}. The flow molecular deformation, represented by tensor Γ_H, is controlled by the macroscopic deformation rates and viscous interactions between the chain and the flowing medium. The linear relations (37) and (38) lead to the well-known linear stress-optical law in the form

$$\langle \mathbf{A}\rangle = \frac{v_0}{5kT}\langle \mathbf{p}\rangle \tag{39}$$

At higher chain deformations, non-linearity of the stress-orientation relationship related to the non-Gaussian chain statistics should be considered.

Molecular anisotropy in the system can be characterized by the deviator of the average orientation tensor

$$\mathbf{D} = \mathrm{dev}\langle \mathbf{A}\rangle = \langle \mathbf{A}\rangle - \frac{1}{3}\mathrm{tr}\langle \mathbf{A}\rangle\mathbf{I} = \frac{2}{3}\begin{bmatrix} f_1 & 0 & 0 \\ 0 & f_2 & 0 \\ 0 & 0 & f_3 \end{bmatrix} \tag{40}$$

Principal components of the deviator, f_i, characterize axial orientation of the statistical segments along the deformation axes. The axial orientation factors read

$$f_1 = \langle A_{11}\rangle - \frac{1}{2}(\langle A_{22}\rangle + \langle A_{33}\rangle) \tag{41}$$

$$f_2 = \langle A_{22}\rangle - \frac{1}{2}(\langle A_{11}\rangle + \langle A_{33}\rangle)$$

$$f_3 = \langle A_{33}\rangle - \frac{1}{2}(\langle A_{11}\rangle + \langle A_{22}\rangle)$$

where the sum

$$f_1 + f_2 + f_3 = 0 \tag{42}$$

The norm of the deviatoric tensor **D**

$$\|\mathbf{D}\| = [\mathrm{tr}(\mathbf{D}\mathbf{D}^{\mathrm{T}})]^{1/2} = \frac{2}{3}\left(f_1^2 + f_2^2 + f_3^2\right)^{1/2} \tag{43}$$

is a scalar measure of the global anisotropy in the flowing system.

Similarly, norm of the average deviatoric stress tensor

$$\|\mathbf{P}\| = \left[\mathrm{tr}(\langle\mathbf{p}\rangle^2) - \frac{1}{3}(\mathrm{tr}\langle\mathbf{p}\rangle)^2\right]^{1/2}$$

$$= \left[\frac{2}{3}\left(\langle p_{11}\rangle^2 + \langle p_{22}\rangle^2 + \langle p_{33}\rangle^2 - \langle p_{11}\rangle\langle p_{22}\rangle - \langle p_{11}\rangle\langle p_{33}\rangle - \langle p_{22}\rangle\langle p_{33}\rangle\right)\right]^{1/2} \tag{44}$$

characterizes intensity of deviatoric stress in the flowing system.

5. Discussion

We consider isochoric biaxial elongational flow, coaxial with the Ox_1, Ox_3 axes of an external coordinate system, where the corresponding velocity gradients are

$$q_1 \neq 0 \quad \text{and/or} \quad q_3 \neq 0; \quad q_2 = -(q_1 + q_3) \tag{45}$$

We refer the flow to uniaxial elongational flow, coaxial with the Ox_3-axis

$$q_1 = q_2 = -\frac{1}{2}q_3 \tag{46}$$

For the uniaxial case, the molecular deformation tensor of the Gaussian chains reads

$$\Gamma_{\mathrm{H}} = \begin{bmatrix} \frac{1}{1+\tau q_3} & 0 & 0 \\ 0 & \frac{1}{1+\tau q_3} & 0 \\ 0 & 0 & \frac{1}{1-2\tau q_3} \end{bmatrix} \tag{47}$$

and the average Gaussian entropy (Eq. (36)) reduces to

$$\frac{\langle S\rangle}{kN} = \text{const.} - \frac{3}{2N}\frac{1-\tau q_3}{1-\tau q_3(1+2\tau q_3)} \tag{48}$$

with the known singularity at $\tau q_3 = 1/2$ which results from infinite extensibility of Gaussian chains. Similar limitation concerns also biaxial deformation of Gaussian chains. The entropy, segmental orientation factor, and stress depends on N and on the reduced elongation rate τq_3 controlling the chain deformation.

In the biaxial flow, the segmental orientation factors are expressed, in the case of Gaussian chains, in terms of the molecular deformation tensor components $1/(1-2\tau q_i)$

$$f_1 = \frac{1}{5N}\left[\frac{1}{1-2\tau q_1} - \frac{1}{2}\left(\frac{1}{1-2\tau q_3} + \frac{1}{1+2\tau(q_1+q_3)}\right)\right] \tag{49}$$

$$f_3 = \frac{1}{5N}\left[\frac{1}{1-2\tau q_3} - \frac{1}{2}\left(\frac{1}{1-2\tau q_1} + \frac{1}{1+2\tau(q_1+q_3)}\right)\right] \tag{50}$$

For the uniaxial flow, the orientation factors reduce to

$$f_3 = \frac{3}{5N}\frac{\tau q_3}{1-\tau q_3(1+2\tau q_3)}, \qquad f_1 = f_2 = -\frac{1}{2}f_3 \tag{51}$$

In the range of higher flow deformations, $\tau q_i \geq 1/2$, the Gaussian model is intractable and leads to undefined stress and orientation characteristics.

Padè approximation of the inverse Langevin function provides a closed-formula approach tractable in the entire range of the reduced flow intensities, τq_i. We use the approach to discuss segmental orientation in the biaxial flow deformation.

Axial orientation factors f_1 and f_3 plotted vs. τq_3, at fixed τq_1 values (indicated), are shown in Figs. 1 and 2 for the

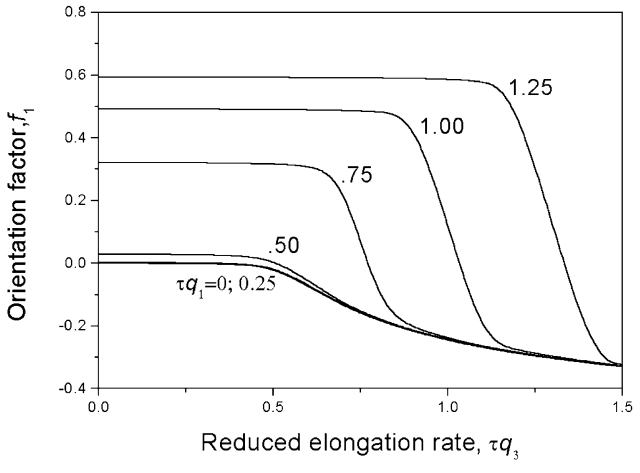

Fig. 1. Axial orientation factor f_1 vs. reduced transversal elongation rate τq_3, at fixed τq_1 values (indicated), computed for biaxial elongational flow of a system of non-Gaussian chains and Padè approximation of the inverse Langevin function. Number of statistical segments in a chain $N = 100$.

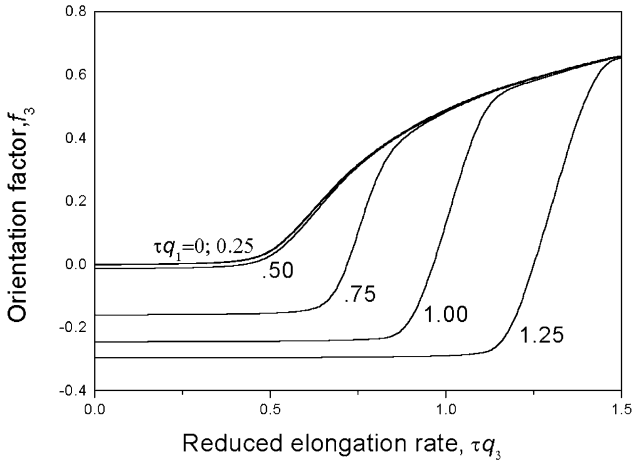

Fig. 2. Axial orientation factor f_3 vs. reduced elongation rate τq_3, at fixed τq_1 values (indicated), for biaxial elongational flow of a system of non-Gaussian chains. Computations as for Fig. 1.

system of non-Gaussian chains subjected to the biaxial elongational flow. Computations are performed using the flow modified inverse Langevin distribution of the chain end-to-end vectors in the Padè approximation (Eq. (3)). The number of statistical segments in each chain is $N = 100$.

Computed axial orientation factors do not show any singularity or discontinuity at $\tau q_i = 1/2$, appearing in the case of Gaussian chain statistics. The orientation factors increase monotonically in the entire range of the stretching rates, τq_1 or τq_3. Upper limit for each of the orientation characteristics is unity indicating ideal axial orientation in the limit of infinite coaxial elongation rate. In the case of affine biaxial stretch, accessible values of the axial orientation factors are considerably lower [11], and do not exceed 0.27 [10,11,18].

As expected, transversal elongational flow τq_3 reduces f_1, and vice versa, τq_1 reduces f_3 (Figs. 1 and 2). The transversal flow becomes effective in reducing the axial orientation factor when its intensity approaches or exceeds the one of the coaxial flow, within a range of about ± 0.25. Below that range, the segmental orientation is not affected by the transversal flow, and f_1 vs. τq_3 plots in Fig. 1 show a plateau. The plateau is the wider, the higher is the coaxial elongation rate τq_1. In the range of strong transversal flow, reducing axial orientation factor, the plots show steep decrease with increasing low intensity. Next, the plot tends to an asymptote, which is mildly converging to a -0.5 value limit, i.e. to an ideal transverse orientation in the limit of infinite transversal elongation rate. The asymptote is common for all values of the coaxial elongation rates. The behavior concerns flow deformations with the reduced elongation rates τq_i, coaxial and transversal, exceeding a value of 0.5. Then, the orientation factors assume the values of about 0.5 indicating high-level axial orientation, or of about -0.25 predicting high transversal orientation of the chain segments.

Within the range of the reduced extension rates below 0.5, the axial orientation factors do not exceed the values of 0.03 for the coaxial and -0.015 for the transversal orientation, indicating much weaker effects in this flow range. Transition to the regime of higher orientations takes place at the reduced stretching rates approaching 0.5, where the Gaussian model shows its singularity.

Discussion of the effective flow orientation in the regime of τq_i above 0.5 requires non-Gaussian chain statistics where the series expansion approach to the chain statistics is practically intractable. In this paper, an approach with the closed-formula Padè approximation of the inverse Langevin function in the non-Gaussian chain statistics is illustrated.

For comparison, the affine biaxial elongation of polymer solids does not show in the range of lower transversal extensions such a wide plateau of the axial orientation factor vs. the transversal deformation plots like in the case of flow deformation. The reduction of the axial orientation of chain segments by the transversal extension takes place in a much wider transversal deformation range, and the decrease of the orientation factor is much milder in the affine case [10,11]. Also any single asymptote, predicted for the case of biaxial extensional flow, is seen at high transverse extensions.

The reduction of the axial orientation factor f_1 by the transversal flow is accompanied by an increase of the axial orientation factor f_3 in the transverse direction, as it is shown in Fig. 2. For $\tau q_1 < 0.5$, an effective orientation in the transverse direction is produced by the transversal flow τq_3 exceeding 0.5. For $\tau q_1 > 0.5$, a steep increase in the transversal orientation is predicted at the transversal flow intensities τq_3 approaching τq_1 value. The transversal flow with distinctly lower intensity is ineffective for producing transversal orientation, the axial orientation factor in the transverse direction is negative in this range, and remains nearly constant vs. τq_3, at fixed τq_1. Above the range of the steep increase, the f_3 vs. τq_3 plots approach the common high orientation asymptote tending to unity with increasing the flow rate to infinity. The picture is complementary to that shown in Fig. 1.

The measure of global orientation anisotropy $\|\mathbf{D}\|$, combining all axial orientation factors, is shown in Fig. 3 vs. τq_3, at fixed τq_1 values. Negligible orientation anisotropy is predicted in the range of the elongation rates τq_3 and τq_1 below 0.5. Higher anisotropy of the segmental orientation requires at least one flow, τq_1 or τq_3, exceeding 0.5. In the range of high flow intensities, $\tau q_1 > 0.5$, effective for segmental orientation, the transversal flow τq_3 practically does not influence the overall anisotropy if its intensity does not exceed the value of τq_1. When the flow intensities coincide, the orientation anisotropy increase monotonically with increasing τq_3 above τq_1, and approaches an asymptotic plot, approximately common for all τq_1 values. Highest values of the orientation characteristic reach a value of about 0.6 (Fig. 3).

The predicted values of the axial orientation and global

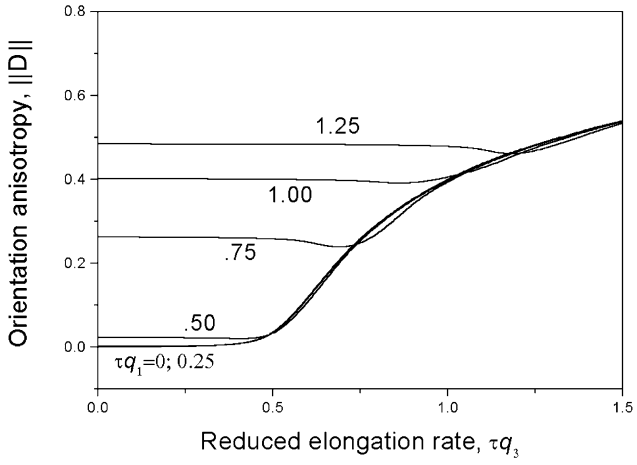

Fig. 3. Global orientation anisotropy $\|\mathbf{D}\|$ vs. transversal elongation rate τq_3, at fixed τq_1 values (indicated), for biaxial elongational flow of non-Gaussian chains. Computations as for Fig. 1.

anisotropy characteristics, f_1, f_2, and $\|\mathbf{D}\|$, are considerably higher for the flow deformation than those computed for the affine biaxial deformation. The values of the anisotropy characteristic in the case of affine deformation do not exceed a value of 0.15 [11].

Fig. 4 shows a deviation of the axial orientation factor f_3 computed using the non-Gaussian model with the Padè approximation from the Gaussian model (Eq. (50)). The comparison is possible in the range of the reduced elongation rates $\tau q_1 < 0.5$ and $\tau q_3 < 0.5$ because of the singularity associated with the Gaussian approach. Significant deviation of the orientation factor from the linear Gaussian plot is evident, even at small values of the orientation factor of the order of 0.01. In the case of affine deformation, the deviation from the Gaussian plot takes place at a higher value of the orientation factor of about 0.1 [11]. This provides another indication that the Gaussian model is inappropriate, particularly for the case of elongational flow deformation, biaxial or uniaxial, although it can be used for not high affine deformations.

The average normal stress differences calculated for the Gaussian system for the case of the biaxial elongational flow read

$$\langle \Delta p^{(3,1)} \rangle \cong \frac{kT}{Nv_0}\left(\frac{1}{1-2\tau q_3} - \frac{1}{1-2\tau q_1}\right) \tag{52}$$

$$\langle \Delta p^{(3,2)} \rangle \cong \frac{kT}{Nv_0}\left(\frac{1}{1-2\tau q_3} - \frac{1}{1+2\tau(q_1+q_3)}\right) \tag{53}$$

and for the uniaxial elongational flow

$$\langle \Delta p \rangle = \langle \Delta p^{(3,1)} \rangle \cong \frac{3kT}{Nv_0}\frac{\tau q_3}{1-\tau q_3(1+2\tau q_3)} \tag{54}$$

The average normal stress differences $\langle \Delta p^{(3,1)} \rangle$ and $\langle \Delta p^{(3,2)} \rangle$, computed for the system of non-Gaussian chain statistics with the Padè approximation are plotted in Figs. 5 and 6, respectively, vs. transversal elongation rate τq_3 at fixed values of τq_1. Both stress differences show a plateau in the range of the transversal flow intensity τq_3 below the value of τq_1. When τq_3 approaches the value of τq_1, the stress differences start to increase steeply with increasing transversal elongation rate. The steep increase is followed by a moderate increase at higher τq_3, asymptotic and common for all τq_1 values. The steep increase takes place in a rather narrow range of the transversal elongation rates.

The maps of the global orientation and stress anisotropy defined by Eqs. (43) and (44) are shown in Figs. 7 and 8, respectively, vs. τq_1 and τq_3. Dashed lines indicate points of the uniaxial elongational flow along x_1x_2 or x_3-axis of the external coordinates system. The maps are symmetrical with respect to the $\tau q_1 = \tau q_3$ line of equally intense biaxial flow

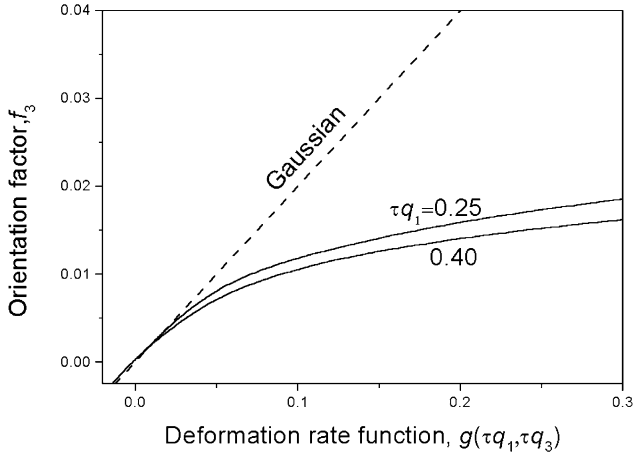

Fig. 4. Axial orientation factor f_3 vs. a deformation rate function $g(\tau q_1, \tau q_3) = (1/N)\{1/(1-2\tau q_3) - [1/(1-2\tau q_1) + 1/(1+2\tau(q_1+q_3))]/2\}$ at fixed τq_1 values (indicated) for biaxial elongational flow of Gaussian (dotted line) and non-Gaussian (solid lines) chains. Computations as for Fig. 1, and the elongation rates limited to the range $\tau q_1 < 1/2$ and $\tau q_3 < 1/2$.

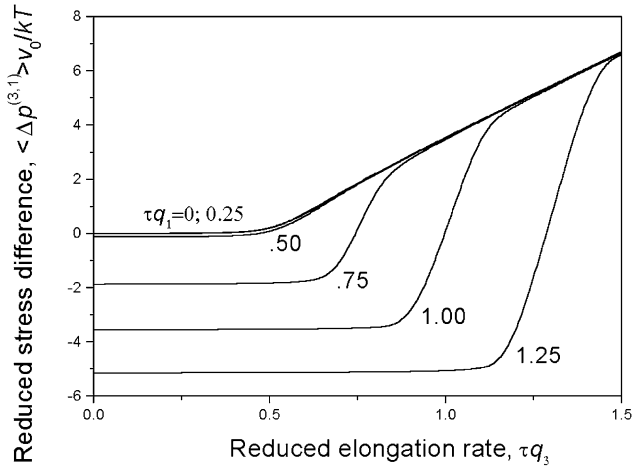

Fig. 5. Reduced, average normal stress difference $\langle \Delta p^{(3,1)} \rangle v_0/kT$ vs. reduced elongation rate τq_3 at fixed τq_1 values (indicated), for biaxial elongational flow of non-Gaussian chains. Computations as for Fig. 1.

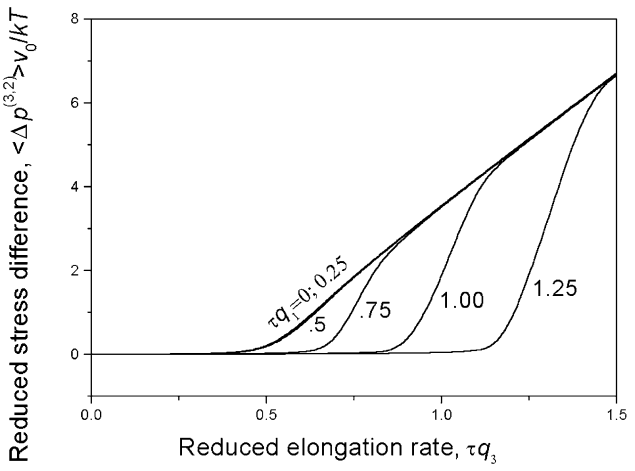

Fig. 6. Reduced difference of normal stresses $\langle\Delta p^{(3,2)}\rangle v_0/kT$ vs. reduced elongation rate τq_3, at fixed τq_1 (indicated), for biaxial, isochoric flow deformation of non-Gaussian chains computed as in Fig. 5.

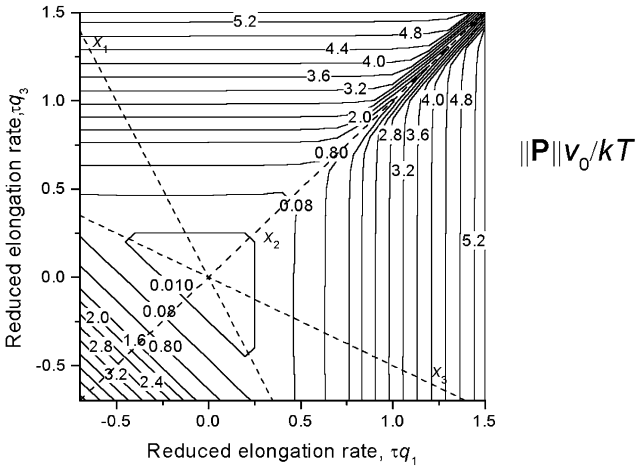

Fig. 8. The map of global dimensionless stress anisotropy $\|\mathbf{P}\|v_0/kT$ in the space of reduced elongation rates τq_1, τq_3 in biaxial elongational flow line as in Fig. 7.

deformation. The maps are similar to the maps obtained for the affine deformation in Ref [11], but with substantially higher values of the orientation characteristics in the case of the flow deformation.

The orientation and stress anisotropy remains practically unaffected by the transversal flow deformation within a wide range of the transversal flow rates below the values of the coaxial flow. This feature is illustrated by nearly vertical lines in the maps within the elongation rate range, with the range being wider, the higher is the value of τq_1. Further increase of τq_3, at fixed τq_1, leads to a transition to the range of horizontal lines in the maps indicating steep and monotonic increase in both, the orientation and stress anisotropy. The maps also indicate the steepest increase in the stress and orientation anisotropy for the uniaxial elongational flows indicated by the dashed straight line intersecting at $\tau q_1 = \tau q_3 = 0$.

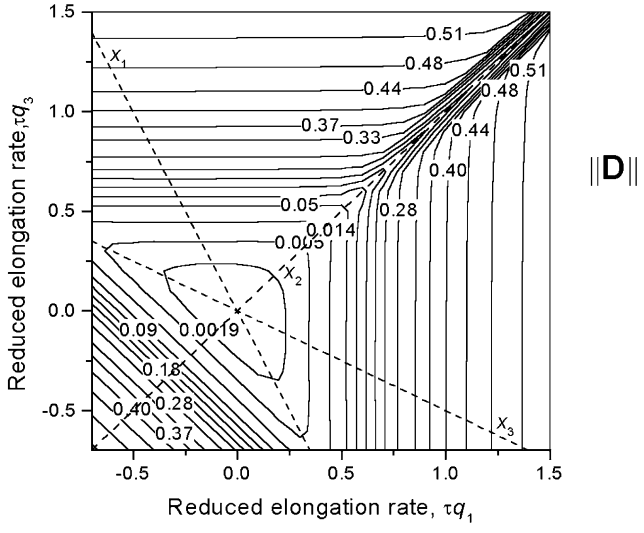

Fig. 7. The map of global orientation anisotropy $\|\mathbf{D}\|$ in the space of reduced elongation rates τq_1, τq_3 for biaxial elongational flow. Dashed straight lines indicate points of uniaxial flow deformation along, respectively, x_1, x_2, and x_3 axes.

6. Conclusions

The Padè approximation of the inverse Langevin function in the non-Gaussian chain statistics leads to a closed-formula theory of segmental orientation and stress in the entire range of chain deformations in the biaxial elongational flow applied to a polymer fluid. Steady-state segmental orientation in the polymer fluid subjected to the flow is controlled by the reduced deformation rates τq_i.

The Gaussian approach and the series expansion approach to the non-Gaussian chain statistics are ineffective in discussing segmental orientation in the biaxial, or uniaxial extensional flows, and lead to singularities, indefinite or poor behavior in the range of deformation rates effective for the orientation.

Steady-state distribution of the chains' end-to-end vectors in the system, as well as average segmental orientation and stress characteristics, are controlled by an equilibrium Boltzmann-type potential which involves the chain elastic free energy and a flow potential controlled by the reduced elongation rates τq_i. In the limit of infinitely long relaxation time, or zero diffusion rate, the chain distribution follows the affine deformation scheme, but the flow deformation theory does not show any continuous transition to the affine deformation model presented in previous paper [11]. We conclude that the segmental orientation, orientation anisotropy, and stress in a viscous, potential flow is controlled by the reduced deformation rates τq_i, while in the case of an affine deformation of a polymer solid by the applied macroscopic deformation.

Segmental orientation and stress behavior in the biaxial

elongational flow resembles the one discussed for the affine deformation in solids, except for much stronger segmental orientations produced in the flow deformation. Elongational flow is much more effective for producing high segmental orientation, axial and global, than the affine elongation applied to solids. The axial orientation factors approach unity in the limit of infinite strain rates τq_i, while for the affine case the upper limit of about 0.27 was found at the highest achievable extensions.

Global orientation and stress anisotropy remains unaffected by the transversal flow if its intensity does not exceed the intensity of the flow in the other direction. One concludes that the orientation and stress anisotropy in biaxial elongational flow is controlled practically by the dominating flow intensity. Transition of the control between the flow directions occur when the flow intensities coincide within a range of about ± 0.25. The transition range is much narrower than in the case of affine deformation in polymer solids.

Acknowledgements

This work was supported in part by Dow Chemical Co., Midland, Michigan (USA). Preliminary results were presented before in the SPE-RETEC Symposium 'Orientation of Polymers', Boucherville, Canada [22].

References

[1] Kashiwagi M, Cunningham A, Manuel AJ, Ward IM. Polymer 1973;14:111.
[2] Cunningham A, Ward IM, Willis HA, Zichy V. Polymer 1974;15:749.
[3] Jarvis DA, Hutchinson IJ, Bower DI, Ward IM. Polymer 1980;21:41.
[4] Ward IM. Adv Polym Sci 1985;66:81.
[5] Bower DI, Jarvis DA, Ward IM. J Polym Sci, Polym Phys Ed 1986;24:1459.
[6] Lapersone P, Tassin JF, Sergot P, Monnerie L, Bourvellec GL. Polymer 1989;30:1558.
[7] Cakmak M, Kim JC. J Appl Polym Sci 1997;65:2059.
[8] Kim JC, Cakmak M, Zhou X. Polymer 1998;39:4225.
[9] White JL, Spruiell JE. Polym Engng Sci 1981;21:850.
[10] Sarac Z, Erman B, Bahar I. Macromolecules 1995;28:582.
[11] Jarecki L, Ziabicki A. Polymer 2002;43:2549.
[12] Ziabicki A. In: Happey F, editor. Applied fibre science, vol. III. New York: Academic Press, 1979. p. 257.
[13] Ziabicki A, Kedzierska K. J Appl Polym Sci 1962;6:111–361.
[14] Cohen A. Rheol Acta 1991;30:270.
[15] Kuhn W, Grün F. Kolloid Z 1941;95:172–307.
[16] Zimm BH. J Chem Phys 1956;24:269.
[17] Ziabicki A. Proceedings of the Fifth International Congress on Rheol, Kyoto, vol. III. University of Tokyo Press, 1970. p. 235.
[18] Ziabicki A, Jarecki L. Colloid Polym Sci 1986;264:343.
[19] Kramers HA. Physica 1944;11:1.
[20] Kramers HA. J Chem Phys 1944;14:415.
[21] Ziabicki A. Fundamentals of fiber formation. London: Wiley, 1976.
[22] Ziabicki A, Jarecki L. Molecular orientation in biaxially deformed polymers. SPE-RETEC Symposium Orientation of Polymers. Boucherville, Canada, September 1998.